A Light-Weight Smartphone GPS Error Model for Simulation

Ali Rostami*, Bin Cheng*, Hongsheng Lu†, John B. Kenney†, and Marco Gruteser*
*WINLAB, Rutgers University, USA
†Toyota Motor North America InfoTech Labs, USA
Email: {rostami,cb3974}@winlab.rutgers.edu, {hongsheng.lu,john.kenney}@toyota.com, gruteser@winlab.rutgers.edu

***Abstract*—This paper proposes a stochastic model for the Global Positioning System (GPS) position errors on smartphones in urban canyons. The need to simulate such errors arises in pedestrian to vehicle communications, for example, which enable a new way to protect vulnerable road users. Studying this technology requires accurate modeling of the GPS precision on portable devices, e.g., smartphones since they share pedestrians' location information with vehicles for collision avoidance. The model is derived from and calibrated with pedestrian GPS traces collected from New York City. We show that the model produces GPS error samples with similar spatial and temporal correlation as in the collected field data.**

***Index Terms*—GPS Error Model, Smartphone, Simulation, V2P.**

I. Introduction

The need to simulate Global Positioning System position traces with their expected positioning errors arises in Pedestrian-to-Vehicle (P2V) communication scenarios that are currently under standardization, for example. Here, Personal Information Devices (PID), such as smartphones, broadcast their kinetic information such as their location, speed, heading, etc. in a Personal Safety Message (PSM) [1]. Nearby vehicles can use the received information to improve their situational awareness, among other Intelligent Transportation System (ITS) applications. While some research questions can be answered experimentally, network scalability questions, that is network performance with hundreds or thousands of nearby transmitters, are often impractical to answer experimentally and studied through simulations.

Simulation is a credible approach for predicting and evaluating system performance at large scales as long as simulator components are carefully modeled and calibrated to reflect their real-world replicas [2]. When evaluating P2V systems using simulations, GPS positioning errors can have a significant impact on the evaluation results, in particular when evaluating accident risk reductions or with context-aware transmissions strategies that are dependent on GPS accuracy [3], [4]. Hence, these simulation environments benefit from accurate GPS position error models.

Previous work focuses more on analyzing sources of error in positioning systems and they often need many details available to accurately account for all of the contributing components. Rankin et al. proposed a GPS error model that accounts for different sources of error [5]. It is among the most sophisticated yet complex models to date that fits more to carefully analyze GPS error rather than simulation purposes. Other examples are map-matching technique [6] and using a 3D map of the environment to reduce the error by considering deflection off of the surrounding buildings [7]. For replicating GPS error in the simulation environment, however, multi-path and low satellite visibility can be considered the primary sources of GPS error, especially in an urban canyon environment. In addition, modeling different sources of GPS error is not a priority in the simulation environment and a realistic combined error model suffices.

Stochastic processes, on the other hand, can be used to model such errors without a need for exact ray-tracing though of satellite signals through a 3D building environment. Ali and Abu-Elkheir [8] have investigated the correlation between consecutive GPS samples as time-series in a vehicular environment. Their measurements, however, is targeting further localization improvements by enabling the GPS device to post-process raw GPS samples using error tracking techniques.

We, therefore, build on such time-series properties to create a GPS error model for smartphones. We further introduce our data collection experiments in Manhattan, New York City, which resulted in 10-hour GPS samples for walking on 7^{th} avenue and 9^{th} avenue. This dataset is used to study the temporal and spatial characteristics of GPS error, as well as comparing different GPS sensors. We then calibrate our introduced GPS error model for different configurations.

In summary, the contributions of this paper are as follows:

- studying characteristics of GPS error such as the correlation between consecutive samples, as well as the distribution of the samples across different environments, times, and sensor models.
- proposing a stochastic GPS error model to capture the extracted characteristics from data analysis via an autoregressive process.
- fitting the proposed model using different subsets of the collected data with different configurations, such as different GPS sensors and different locations. The fits are location-specific.

II. GPS Error Model

In this section, we study a trace of consecutive GPS samples and model the offset of the recorded samples from their true location, i.e. their ground truth.

A. Problem Definition

The measured location $\vec{s}$ = (s_{lat},s_{lon}) at time t can be modeled as a summation of the actual (ground truth) position, i.e. $\vec{g}$ = (g_{lat},g_{lon}), and an error term $\vec{e}$ = (e_{lat},e_{lon}), as shown in Eq. 1. Note that we focus on modeling two-dimensional positions, therefore the actual position and the error (the offset of the reported position by the sensor from the ground truth) have two components which we will refer to as latitude and longitude.

$$\vec{s}(t) = \vec{g}(t) + \vec{e}(t) \tag{1}$$

In a simulation environment, the actual locations of the receivers' antennas $\vec{g}$ at any given time t are determined by a separate mobility model. The focus of this work is on modeling the offsets from the ground truth $\vec{e}$.

In particular, we seek a stochastic model that accurately represents the direction and the magnitude of the error as well as their changes over time.

B. Autoregressive Model

To address this, we model the GPS error $\vec{e}$ through an autoregressive (AR) process. This is motivated by empirical observations that the GPS error term of successive samples has high autocorrelation. Fig. 1 shows the autocorrelations between longitudinal and latitudinal errors with one second delay between consecutive samples. As evident, the autocorrelation is high for the first few lags. Hence, an AR process is a suitable model.

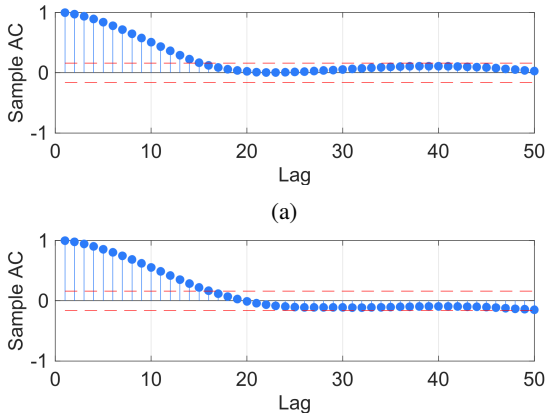

Fig. 1: Autocorrelation samples for the error magnitude of one of the GPS traces collected from 9th Avenue; (a) Longitudinal errors, and (b) Latitudinal errors.

Eq. 2 shows how the error term can be represented through an AR process of order p.

$$\vec{e}(t) = \vec{\delta} + \sum_{i=1}^{p} \vec{\phi_i}\vec{e}(t-i) + \vec{w}(t) \tag{2}$$

Here, t is the t^{th} sample in the time-series, $\vec{\phi_i}$ is a vector of AR parameters for the i^{th} lag, $\vec{w}$ is a vector of zero-mean white noises with standard deviation $\vec{\sigma_w}$, and $\vec{\delta}$ is a constant vector as defined in Eq. 3.

$$\vec{\delta} = (1 - \sum_{i=1}^{p} \vec{\phi_i})\vec{m} \tag{3}$$

Here $\vec{m}$ is a vector containing the mean of longitudinal and latitudinal errors.

C. Degree of the Autoregressive Process

We determine the degree p, of such an AR process as follows. Let $p \in \mathbb{N}$ be the maximum distant lag that has a significant impact on the times series behavior. p is calculated using the Partial Autocorrelation Function (PAF).

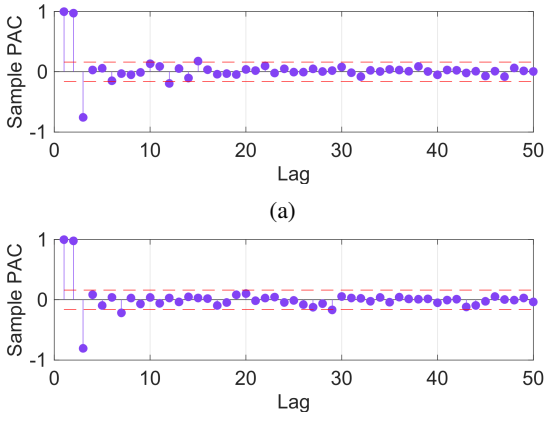

Fig. 2: Partial Autocorrelation samples for a GPS trace collected from 9th Avenue; (a) Longitudinal and (b) Latitudinal errors.

Fig. 2 shows the resulting partial autocorrelation samples using both the longitudinal and latitudinal errors for one of the traces. The red dashed lines are the confidence thresholds. Lags with values between these thresholds do not have a major impact on the precision of the fit. These lags, however, can still be considered in the model.

As seen in Fig. 2, the result of applying PAF on the longitudinal/latitudinal errors shows that the first three lags have a significant impact on the behavior of the stochastic process. Therefore, we use an AR process of degree three ($p = 3$ in Eq. 2). The observed significance values were approximately similar when other traces were examined as well.

III. Model Calibration

The proposed model in the previous section leverages the characteristics of time-series. This model can be calibrated to mimic the properties of provided GPS samples by smartphones in a particular environment. The model fits, however, will be location-specific. In this section, we report on our data collection campaign in New York City. The collected GPS traces are further analyzed and used for calibration of the GPS error model. We particularly intend to fit the proposed model for $\vec{\delta}$, $\vec{\phi_1}$, $\vec{\phi_2}$, $\vec{\phi_3}$, and $\vec{\sigma_w}$ of the white noise $\vec{w}$ in Eq. 2.

A. Data Collection

GPS traces are collected during two afternoons in Manhattan, New York City. We developed an Android app which uses the standard Android API to retrieve raw GPS readings from the smartphone's GPS sensor and records them in a CVS file. The app records latitude, longitude, heading, speed, number of visible GPS satellites to the phone, and the estimated error, as well as the timestamp of the recording time. Two smartphones are used at the same time to collect the samples: 1) a Google Pixel smartphone (1st generation) with Qualcomm Snapdragon 821 chipset, and 2) a Nexus 5 smartphone with Qualcomm Snapdragon 800 chipset. These two smartphones use different integrated GPS sensors.

To collect the required GPS samples, one of the authors walked in predefined routes on the map (we call it a trip), on the sidewalks and tried to maintain pace (See Fig. 3 for two example trips). He further recorded time by pressing a button on each of the smartphones' screens once at the beginning of the trip, and afterward, when arriving at certain locations along his walking path–right before entering the crosswalks on his path. That makes 16 landmarks for one trip. The coordination of each landmark was obtained from Google Earth. Given the assumption of constant speed of the person between each pair of landmarks and the recorded arrival timestamps, the ground truth for each logged GPS sample was approximated. While not perfect, the measurement error appears to be acceptable. In the end, over 19k processed samples were available in 25 different trips.

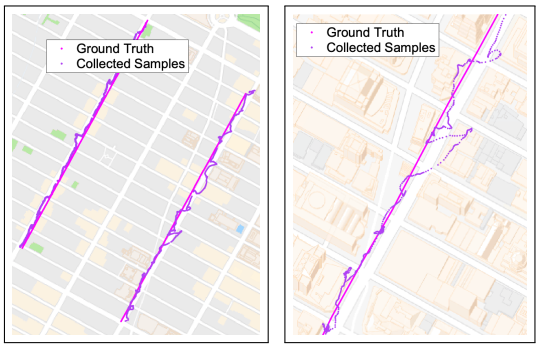

(a) (b)

Fig. 3: (a) Examples of collected GPS samples using Pixel phone and their corresponding estimated ground truth for 7th and 9th Avenues, Manhattan, NYC, and a (b) zoomed-in on the 7th avenue.

Fig. 3 shows two out of several collected GPS traces. The depicted samples belong to Manhattan's 7th and 9th avenues. Each magenta dot shows a recorded GPS location by the smartphone's GPS sensor and the time interval between two consecutive samples is one second.

B. Calibration

After approximating the amount of error for each collected GPS sample in the dataset, the magnitude of errors are studied from three different perspectives: 1) spatial, where the collected GPS samples from two different environments on the map are compared, 2) temporal, where the GPS samples are collected from the same route on the map using the same phone on different days, and 3) different sensor types, where two different phones with different GPS sensor chipset are used to simultaneously collect data on the same route. Note that for the spatial comparison, the samples from different routes on the map are not collected exactly at the same time and that could impact the results.

TABLE I: Information of the Datasets

Dataset	Route	Device
DS1	9th Avenue	Nexus 5
DS2	9th Avenue	Pixel (1st generation)
DS3	9th Avenue	Pixel (1st generation)
DS4	9th Avenue	Pixel (1st generation)
DS5	7th Avenue	Pixel (1st generation)
DS6	9th Avenue	Pixel (1st generation)
DS7	7th Avenue	Nexus 5

Table I shows the details of the available datasets such as the route that the data is collected, as well as the device which the data is collected with. These datasets are used for comparing the behavior of the positioning accuracy temporally, spatially, and across different GPS receivers.

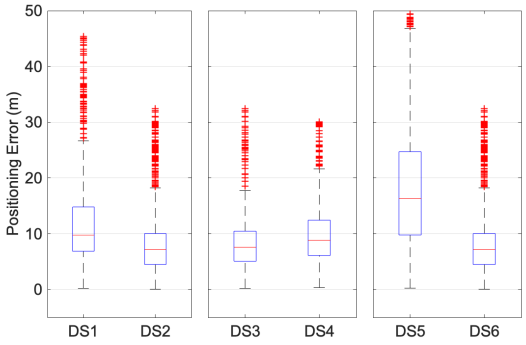

Fig. 4: Statistical comparison between: (left) collected samples using different GPS sensors, (middle) temporally different, and (right) spatially different datasets.

Fig. 4 shows a statistical comparison between different subsets of the entire collected data from the Manhattan area. The leftmost figure shows the comparison between different sensors by comparing positioning error distribution for the data collected on 9th avenue. DS1 is the concatenated data using the Nexus 5 smartphone, and DS2 shows, as well, the concatenated data collected using the Pixel smartphone. The figure in the middle, further shows the temporal comparison of the error distribution. This figure compares the statistical distribution of the positioning error for the samples collected on 9th avenue at different times using Pixel smartphone. The rightmost figure shows the spatial comparison of the error distribution, by comparing GPS error from 7th avenue (DS5) and 9th avenue (DS6) using the Pixel smartphone.

One observation from the distribution of different datasets in Fig. 4 is that the impact of the environment is higher than

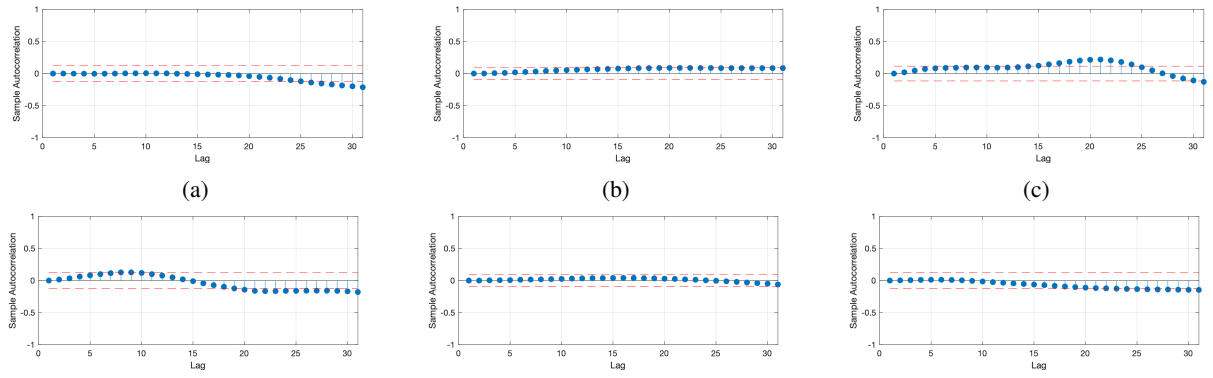

Fig. 5: Difference of autocorrelation samples between the simulated traces and collected GPS traces; Longitudinal error (1st row) and latitudinal error (2nd row) for DS1 (1st column), DS5 (2nd column), and DS6 (3rd column).

the others. DS5 represents a dataset collected in 7th avenue, where the area is surrounded by many skyscrapers among the tallest in the world. On the contrary, the environment of DS6 is mostly surrounded by <8-story buildings, providing much more clear sky view for the GPS sensors. Another observation is that the Pixel phone generally does better than the Nexus 5 phone, both in terms of the expected error magnitude and amount of variations. By comparing DS3 and DS4, we can also confirm the impact of time on the positioning accuracy, which is mostly because the visible set of GPS satellites to the smartphone is time-varying.

We fit the model for the aforementioned data by Yule-Walker estimation method [9]. The estimation and calculation are carried out by MATLAB. Table II shows the fitted parameters for several different datasets.

TABLE II: Fitted $AR(3)$ parameters

	Err.	δ	ϕ_1	ϕ_2	ϕ_3	σ_w
DS5	e_{lat}	0.07	1.18	−0.06	−0.14	1.52
	e_{lon}	−0.02	1.15	−0.03	−0.14	1.58
DS2	e_{lat}	0.03	1.31	−0.04	−0.28	0.49
	e_{lon}	−0.02	1.66	−0.72	0.04	0.39
DS1	e_{lat}	−0.02	1.71	−0.75	−0.04	0.72
	e_{lon}	0.02	1.52	−0.53	−0.07	0.93
DS7	e_{lat}	0.02	1.58	−0.53	−0.06	0.53
	e_{lon}	−0.11	1.23	−0.15	−0.1	0.99

Table II shows the fitted parameters for the resulting AR process for 7th and 9th avenues for both smartphones. Note that the parameters only show the fit for one of several data collection passes with the same configuration, i.e. without concatenating all passes with similar configurations. We believe higher simulation accuracy is achievable if the fitting procedure is done for smaller sections of the map other than for the entire trace.

IV. Cross-Validation

The calibrated model is implemented in ns-3 network simulator [10] to simulate GPS traces for comparison. In this section, the goodness of fit is examined by comparing the simulated samples and the collected GPS samples from the experiments regarding different characteristics of a time-series.

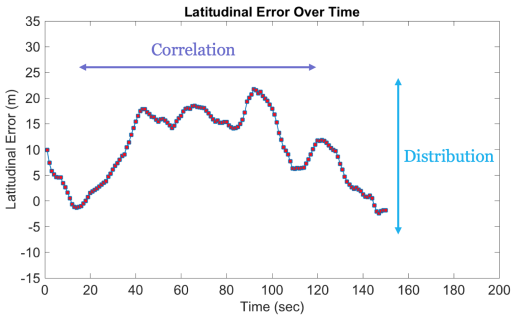

Fig. 6: A time-series with its two primary characteristics marked.

The key metrics we use to evaluate the fit of the time-series of position errors are the overall distribution of error vectors and the correlation of error vectors over time, as illustrated in Fig. 6.

For cross-validating, the correlation between different lags, the movement of the person who collected the data was replayed in the simulator. For each simulated trip, the corresponding fit for the same trip was chosen from Table II. The result was three GPS traces of similar length to one trip during the data collection. The steps towards calibrating the model were repeated for each simulated trace. Then, we calculated the offset of the autocorrelation between the simulated traces for each fit and the GPS trace which was used to create that fit. Fig. 5 illustrates the resulted values for cross-validating the calibrated model for each fit in terms of autocorrelation offset. As seen, most of the fits have negligible noise for the most significant lags, i.e. smaller values on the x-axis for both the longitudinal and latitudinal errors.

For examining the goodness of fit for the distribution of the generated samples, Quantile-Quantile plot (QQPlot) is a widely accepted way to compare the distribution of two datasets together. In this context, we compare the distribution of the generated GPS traces using different fits from Table II with the corresponding datasets. Note that the fitted model is sensitive to time as well. Given that, we do not cross-

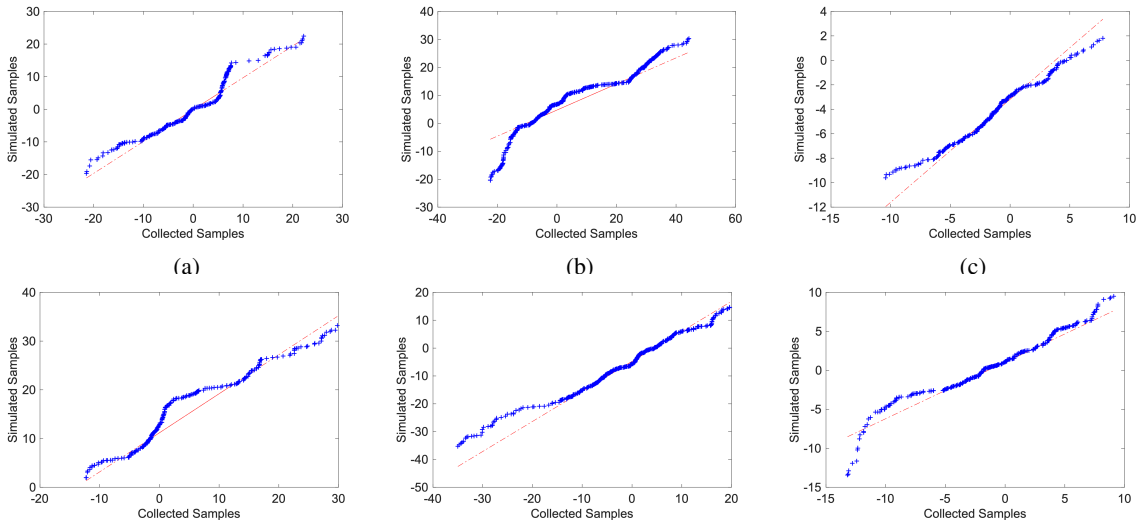

Fig. 7: Quantile-quantile comparison between the simulated traces and collected GPS traces; Longitudinal error (1st row) and latitudinal error (2nd row) for DS1 (1st column), DS5 (2nd column), and DS6 (3rd column).

validate an individual fitted parameter set with other datasets. Fig. 7 shows that the distribution of DS7 is a bit noisier than the rest. Note that the Manhattan area is an urban canyon with a very limited sky view. In addition, occasional signal blocks are usual when walking in the sidewalks when passing construction zones with the temporary safety ceiling. All in all, the amount of noise in the samples seems acceptable.

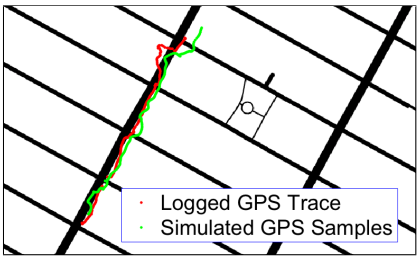

Fig. 8: Zoomed-in map with logged GPS trace and simulated GPS samples using the calibrated GPS error model.

To illustrate the performance of the proposed GPS error model for the 9th Avenue, the model is implemented in both MATLAB and ns-3. Fig. 8 shows the logged GPS trace in a tight train of red dots, and the train of green dots for the simulated GPS samples by adding the generated errors by the calibrated $AR(3)$ model to the ground truth.

V. Conclusion

In this paper, we collected several GPS samples and calculated the magnitude of error for each sample via ground truth approximation. We further analyzed the GPS error as a time-series and modeled it using autoregressive (AR) process and calibrated the model using the collected data from New York City. The model is calibrated for different configurations. We further cross-validated the fits with the collected data to show the goodness of fit in terms of the correlation between different time lags, as well as the distribution of the simulated traces. It is shown that the time correlation offset does not exceed the significance threshold for the important lags and that the simulated traces show a similar distribution to the collected samples.

References

[1] SAE J2945/9. Performance Requirements for Safety Communications to Vulnerable Road Users. March 2016.

[2] Byungkyu Park and JD Schneeberger. Microscopic simulation model calibration and validation: case study of vissim simulation model for a coordinated actuated signal system. *Transportation Research Record*, 1856(1):185–192, 2003.

[3] Ali Rostami, Bin Cheng, Hongsheng Lu, John B Kenney, and Marco Gruteser. Performance and channel load evaluation for contextual pedestrian-to-vehicle transmissions. In *Proceedings of the First ACM International Workshop on Smart, Autonomous, and Connected Vehicular Systems and Services*, pages 22–29. ACM, 2016.

[4] Ali Rostami, Bin Cheng, Hongsheng Lu, Marco Gruteser, and John B Kenney. Reducing unnecessary pedestrian-to-vehicle transmissions using a contextual policy. In *Proceedings of the 2nd ACM International Workshop on Smart, Autonomous, and Connected Vehicular Systems and Services*, pages 3–10. ACM, 2017.

[5] James Rankin. Gps and differential gps: an error model for sensor simulation. In *Position Location and Navigation Symposium*, pages 260–260, 1994.

[6] James Murphy and Yuanyuan Pao. Map matching when the map is wrong: Efficient vehicle tracking on-and off-road for map learning. *arXiv preprint arXiv:1809.09755*, 2018.

[7] Li-Ta Hsu, Yanlei Gu, and Shunsuke Kamijo. 3d building model-based pedestrian positioning method using gps/glonass/qzss and its reliability calculation. *GPS solutions*, 20(3):413–428, 2016.

[8] Najah Abu Ali and Mervat Abu-Elkheir. Improving localization accuracy: Successive measurements error modeling. *Sensors*, 15(7):15540–15561, 2015.

[9] Benjamin Friedlander and Boaz Porat. The modified yule-walker method of arma spectral estimation. *IEEE Transactions on Aerospace and Electronic Systems*, (2):158–173, 1984.

[10] ns-3. https://www.nsnam.org/.